NEOPLASIA
www.neoplasia.com

Volume 14 Number 3 March 2012 pp. 206–218 206

Single Nucleotide Polymorphism Microarray Analysis in Cortisol-Secreting Adrenocortical Adenomas Identifies New Candidate Genes and Pathways[1,2]

Cristina L. Ronchi[*,3], Ellen Leich[†,3], Silviu Sbiera[*], Dirk Weismann[*], Andreas Rosenwald[†], Bruno Allolio[*] and Martin Fassnacht[*]

*Unit of Endocrinology, Department of Internal Medicine I, University Hospital of Würzburg, Würzburg, Germany; [†]Department of Pathology, University of Würzburg, Würzburg, Germany

Abstract

The genetic mechanisms underlying adrenocortical tumor development are still largely unknown. We used high-resolution single nucleotide polymorphism microarrays (Affymetrix SNP 6.0) to detect copy number alterations (CNAs) and copy-neutral losses of heterozygosity (cnLOH) in 15 cortisol-secreting adrenocortical adenomas with matched blood samples. We focused on microalterations aiming to discover new candidate genes involved in early tumorigenesis and/or autonomous cortisol secretion. We identified 962 CNAs with a median of 18 CNAs per sample. Half of them involved noncoding regions, 89% were less than 100 kb, and 28% were found in at least two samples. The most frequently gained regions were 5p15.33, 6q16.1, 7p22.3-22.2, 8q24.3, 9q34.2-34.3, 11p15.5, 11q11, 12q12, 16q24.3, 20p11.1-20q21.11, and Xq28 (≥20% of cases), most of them being identified in the same three adenomas. These regions contained among others genes like *NOTCH1*, *CYP11B2*, *HRAS*, and *IGF2*. Recurrent losses were less common and smaller than gains, being mostly localized at 1p, 6q, and 11q. Pathway analysis revealed that Notch signaling was the most frequently altered. We identified 46 recurrent CNAs that each affected a single gene (31 gains and 15 losses), including genes involved in steroidogenesis (*CYP11B1*) or tumorigenesis (*CTNNB1*, *EPHA7*, *SGK1*, *STIL*, *FHIT*). Finally, 20 small cnLOH in four cases affecting 15 known genes were found. Our findings provide the first high-resolution genome-wide view of chromosomal changes in cortisol-secreting adenomas and identify novel candidate genes, such as *HRAS*, *EPHA7*, and *SGK1*. Furthermore, they implicate that the Notch1 signaling pathway might be involved in the molecular pathogenesis of adrenocortical tumors.

Neoplasia (2012) 14, 206–218

Introduction

Adrenocortical tumors are among the most frequent human neoplasias with an overall prevalence of 2% in the general population [1]. They mostly consist of benign adrenocortical adenoma (ACA), whereas adrenocortical carcinomas (ACC) are rare aggressive tumors with a poor prognosis [2]. The genetic mechanisms underlying adrenocortical tumor development are still largely unknown. In particular, it is still unclear if ACCs evolve from ACAs after a second-hit paradigm. Although such a sequence has been occasionally observed [3], long-term follow-up of incidentally discovered adrenocortical neoplasms suggests that ACA in general maintain a benign phenotype [4]. Adrenocortical tumors can be either endocrinologically silent or hormonally active. It has been postulated that autonomous hormone production in ACA may be associated with increased expression of enzymes needed for corticosteroid production along with alterations in transcription factors that enhance

Abbreviations: ACA, adrenocortical adenoma; ACC, adrenocortical carcinoma; CGH, comparative genomic hybridization; CNA, copy number alteration; cnLOH, copy-neutral loss of heterozygosity; FISH, fluorescence *in situ* hybridization; LOH, loss of heterozygosity; qRT-PCR, quantitative real-time polymerase chain reaction; SNP, single nucleotide polymorphism; UPD, uniparental disomy

Address all correspondence to: Cristina L. Ronchi, MD, PhD, Unit of Endocrinology, Department of Internal Medicine I, University Hospital, University of Würzburg, Oberrduerrbacher-Strasse 6, 97080 Würzburg, Germany. E-mail: cry_ronchi@yahoo.it, Ronchi_C@klinik.uni-wuerzburg.de

[1]This work was supported by grants of the Deutsche Krebshilfe (grant 107111 to M.F.) and the Deutsche Forschungsgemeinschaft (grant FA466/3-1 to M.F.). It was also supported by the Alexander von Humboldt Foundation (C.L.R.). The authors disclose no commercial affiliations or financial interests that may be considered conflicts of interest regarding this article.

[2]This article refers to supplementary materials, which are designated by Tables W1 to W4 and Figures W1 to W4 and are available online at www.neoplasia.com.

[3]These authors contributed equally to this article.

Received 16 December 2011; Revised 13 February 2012; Accepted 13 February 2012

DOI 10.1593/neo.111758

the expression of steroid-metabolizing enzymes [5]. However, the molecular mechanisms responsible for hormone overproduction are not well understood. Because autonomous cortisol hypersecretion is *per se* associated with serious morbidity and increased mortality [6], a better understanding of its pathogenesis might lead to new treatment strategies.

Molecular studies of the inherited syndromes with increased ACC risk coupled with recent advances in genomic and expression profiling, have helped to improve our understanding of the genetic mechanisms underlying adrenocortical tumor development [7–9]. For instance, microsatellite markers revealed common inactivating mutations or loss of heterozygosity (LOH) at 17p13, a region that includes the *TP53* tumor suppressor gene, LOH at 11q13 and 2p16, and alterations of the imprinted 11p15 locus (paternal isodisomy) leading to IGF2 overexpression in ACC [7,10]. In addition, a constitutive activation of the Wnt/β-catenin signaling pathway is common in both ACA and ACC, being likely involved in both adrenocortical development and neoplasia [11–13]. Nevertheless, with few exceptions, the molecular candidates so far proposed as diagnostic or prognostic markers have not been validated in subsequent studies, mostly due to different methodological approaches and heterogeneity of the tumor. Copy number alterations (CNAs) have been described in adrenal hyperplasia, ACA and ACC using fluorescence *in situ* hybridization (FISH), karyotyping, and either conventional comparative genomic hybridization (CGH) [14–18] or array-based CGH [19,20]. In particular, losses at 1p, 2q, 3p, 6q, 9, 11, 17p, and 18q and gains at 4, 5, 12q, 16, 19, and 20q have been reported in patients with sporadic ACC, demonstrating large genetic derangements, often involving previously undescribed pathomechanisms [21]. However, results from CGH studies have been highly variable and restricted to very large regions containing too many genes to allow identification of specific candidate genes associated with disease initiation or progression. In addition, CGH cannot detect other chromosomal changes such as LOH.

Single nucleotide polymorphism (SNP) microarrays provide a useful method, which allows detecting not only genome-wide copy number (CN) data at high resolution but also LOH events [22]. Merging these two analyses, it is also possible to identify copy-neutral LOH (cnLOH or uniparental disomy [UPD]), a previously underestimated chromosomal defect which comprises 50% to 70% of LOH events detected in human tumors [23]. Furthermore, recent SNP array platforms, such as Affymetrix SNP 6.0, often identify amplifications/deletions at a single gene level, which could not have been accomplished by previous methods. Thus, modern SNP arrays offer a powerful and increasingly popular method for oncogene and tumor suppressor gene discovery, as well as for cancer classification [24].

In the present study, we used high-resolution SNP arrays for the first time to investigate genetic events involved in the pathogenesis of adrenocortical tumors. We selected benign cortisol-secreting tumors with matched blood samples in a paired analysis approach to restrict tissue heterogeneity and to allow improved detection of tumor specific events. Our aim was to discover new candidate genes involved in early tumorigenesis and/or autonomous cortisol secretion.

Materials and Methods

Study Population

A total of 18 cortisol-secreting ACAs with matched normal peripheral blood samples were selected for the present study. Clinical parameters, such as sex, age at diagnosis, date of surgery, tumor size, pathologic classification, and results of hormone analysis were collected from patient records. Specifically, baseline morning serum cortisol and plasma corticotrophin levels, cortisol concentrations after dexamethasone suppression test (1 mg, 23.00 hours), 24-hour urinary free cortisol excretion, and midnight serum or salivary cortisol levels were considered. Malignancy was excluded according to recognized clinical, biochemical, and morphologic criteria. The biochemical diagnosis of cortisol hypersecretion was made according to established criteria [25]. Subclinical hypercortisolism was defined according to the following criteria: postdexamethasone cortisol levels greater than 5 μg/dl, corticotrophin levels less than 25 pg/L and at least one additional pathologic test among 24 hours urinary free cortisol and midnight serum or salivary cortisol levels in the absence of typical clinical features of Cushing syndrome [26]. Clinical sequelae of cortisol excess were also taken into account (i.e., arterial hypertension, diabetes mellitus, and osteoporosis). The study was approved by the ethical committee of the University of Würzburg (permit no. 93/02), and written informed consent was obtained from all patients.

Tissue Samples and DNA Extraction

Tumor tissue specimens collected from patients operated between 1995 and 2010 were used for the present study. Corresponding peripheral blood samples were also taken from all patients. Tumor and blood samples had been stored at −80°C in our Department (University Hospital, Würzburg, Germany). Genomic DNA from both frozen tumor and blood samples was extracted using standard procedures (QIAamp DNA Mini and Blood Mini; Qiagen, Valencia, CA). Only samples with appropriate DNA quality as measured by the ratio of absorbance at 260 to 280 nm ($A_{260}/A_{280} \geq 1.8$) using the Bioanalyzer (Agilent Technologies, San Jose, CA) were further evaluated.

SNP Arrays

SNP array experiments were performed using the high-resolution Affymetrix GeneChip Human Mapping 6.0 microarray (SNP 6.0; Affymetrix, Inc, Santa Clara, CA) containing 906,600 probes for SNPs and 946,000 probes for CNVs, with a median physical intermarker distance of 680 bp. Briefly, 250 ng of genomic DNA was digested with *Nsp*I and *Sty*I (New England Biolabs, Inc, Ipswich, MA), respectively, and then ligated to Nsp or Sty adaptors. The adaptor-ligated DNA fragments were amplified, fragmented using DNase I, end labeled with a biotinylated nucleotide, and hybridized to a human SNP 6.0 array (Affymetrix) at 49°C for 17 hours. After hybridization, the arrays were washed, stained, and finally scanned with a GeneChip Scanner 3000 7G (Affymetrix). All procedures were performed according to the manufacturer's protocols.

SNP Arrays Data Analysis

Affymetrix raw intensity data (.CEL files) were generated by the command console and quality control (QC) was assessed by the Genotyping Console software (GTYPE version 4.0; Affymetrix). Only arrays were accepted that had a QC of 1.7 or higher and a MAPD of 0.3 or smaller, as recommended for large study sets.

CN analysis was performed using the Partek Genomics Suite software package, Version 6.5 (Partek GS; Partek, Inc, St. Louis, MO). In particular, .CEL files were imported into the Partek GS and normalized to baseline reference intensities using the robust multichip

average algorithm. A preliminary unpaired data analysis was performed in all 18 ACAs and 18 blood samples. Unexpectedly and for no obvious reasons, three blood samples showed a large number of CNAs. Similar results were obtained after repeated blood sampling, hybridization and data analysis. Therefore, it was decided to exclude these samples from further analysis. The paired CNA analysis was then carried out by comparing each intensity of the hybridization signal from a tumor sample to that of the matched normal lymphocyte DNA. A log ratio calculation was carried out to determine the relative intensity and the log ratios were then turned into CN space using the following formula: $CN = 2 \times 2^{(\log 2 \text{ intensity})}$. Regions of CNAs were detected by a genomic segmentation algorithm to characterize isolated islands of significantly higher- or lower-intensity ratios into CNA regions [27]. Delineating CNA and its boundaries can often be challenging [28]. To reduce the detection of false-positive alterations owing to inherent microarray "noise" and to achieve a balance between sensitivity and specificity, we used the following parameters: a minimum of 10 markers (defining the smallest detectable region), a P threshold of .0001 (controlling for outlying probes), a signal-to-noise ratio of 0.6 [27], and an expected range of ±0.5 (distance from normal CN). Accordingly, regions with a CN score greater than 2.5 or less than 1.5 were considered as gains or losses, respectively. A false discovery rate–based adjustment was always applied and performed using the step up method with an alpha value of 0.05 [29]. CNAs detected by genomic segmentation were visually verified using the Partek Genome Browser. Figure W1 gives an example how the genomic segmentation algorithm is able to specifically detect regions of gains and losses.

Genotype analysis was performed using the Birdseed v2 algorithm provided by the Affymetrix GTC (version 4.0), according to the recommended guidelines. The SNP call rate after genotype analysis was greater than 95% in all samples. For the LOH analysis, CHP files were imported into the Partek GS and the hidden Markov model algorithm was applied. The SNP calls made by the software were AB (heterozygous SNP), AA and BB (homozygous SNP), and no call (if the software was unable to decide on the calls). LOH was assumed when the normal tissue biallelic marker (AB) was found to be monoallelic in tumor tissue. The heterozygosity rate was calculated as the number of AB calls/total number of calls, where low heterozygosity rate implies LOH (frequency of heterozygous calls for a normal region = 0.3). The LOH data were merged with CNAs to obtain the cnLOH. In fact, LOH events can be accompanied by allele gains (AAA or BBB) or losses (A0 or B0) or can be defined as cnLOH when they are not associated with CNAs (AA or BB).

The Partek workflow and the Hg19 (reference file) were used for the gene annotation (RefSeq). The observed CNAs were checked against the database of genomic variants (dBVar). Gene ontology enrichment and gene family analysis of gene sets was performed using the gene set enrichment analysis (GSEA) annotation tool. The relevance of altered genes to currently known canonical pathways was investigated using the MetaCore Analytical suite (Pathways Maps; GeneGo, Inc, Thomson Reuters, St Joseph, MI). In particular, MetaCore was used to calculate the statistical significance (P value) of the probability of assembly from a random set of nodes (genes) of the same size as the input list (single experiment analysis). $P < .02$ indicates a statistically significant nonrandom association. The same software was used to characterize the gene networks.

To quantify the known and predicted protein-protein interaction properties, we used the search tool for the retrieval of interacting genes/proteins (STRING, Version 9.0) database of direct (physical) and indirect (functional) interactions [30]. The interactions are derived from genomic content, high-throughput experiments, coexpression, and previous knowledge [31]. A high confidence score of 0.700 was chosen.

Correlation to Clinical Data

The comparison of clinical parameters, such as age at diagnosis, tumor size, and hormonal secretion pattern, between groups with or without genetic alterations was performed by appropriate statistical methods. The Fisher exact test or the χ^2 test was used to investigate the relationship between dichotomic variables, whereas a one-way analysis of variance model or a two-sided t test was used to test continuous variables. Correlations between different parameters were evaluated by linear regression analysis. Statistical analyses were made using GraphPad Prism (version 4.0; La Jolla, CA) and SPSS Software (PASW Version 19.0; SPSS, Inc, Chicago, IL). $P < .05$ was considered statistically significant.

FISH Analysis

Selected CNAs identified by SNP array results were validated on 13 available paraffin-embedded tumor tissue samples using FISH analysis according to previously published methods [32]. Specifically, we investigated two chromosomal regions, one with a gain and one with a loss according to the SNP analysis (11p15.5 and 6q23.2, respectively). BAC clones (Children's Hospital Oakland Research Institute) were used and hybridized together with the corresponding centromere-specific reference probe (Vysis; Abbott Molecular, Abbott Park, IL). The probes chosen for the gained region 11p15.5 were specific for the *IGF2* locus (RP11-373H8, RP11-72D6) and those chosen for the lost region 6q23.2 were specific for the *serum glucocorticoid kinase 1* (*SGK1*) locus (RP11-325G4, RP11-692B5, RP11-466N7). A total of 100 interphase nuclei were analyzed with Zeiss Axioskop 2 Microscope (Carl Zeiss MicroImaging) by two independent operators, and a ratio of red signals to green signals was calculated. The cutoff for defining gains or losses was more than 40% cells.

Quantitative Real-time Polymerase Chain Reaction

CN validation. Quantitative real-time polymerase chain reaction (qRT-PCR) analysis was performed on DNA samples to validate the CN status of selected genes that were found to be altered using SNP arrays. The corresponding blood samples were used as calibrators. Primers for the genes *IGF2*, *EPHA7*, *CYP11B2*, *CTNNB1*, and *SGK1* were designed using the Ensembl database and the primer BLAST tool (NCBi; Table W1). The SYBR Green kit (qPCR Supermix; Invitrogen, Karlsruhe, Germany), the C1000 Thermal Cycler (CFX96 real-time system; Biorad, Hercules, CA), and the Bio-Rad CFX Manager (Version 2.0) were used. Twenty nanograms of DNA was used in each qRT-PCR, and all samples were run in duplicates. The conditions for amplifications were 95°C for 3 minutes followed by 40 cycles of 95°C for 15 seconds, 62°C for 15 seconds, and 72°C for 15 seconds, followed by melting temperature curve analysis. CNAs were assessed by relative quantification methods, using *GAPDH* as endogenous reference, and were calculated as follows: $2 \times 2^{[(Dt - DGAPDH) - (Nt - NGAPDH)]}$, where D_t is the mean threshold cycle number for experimental primer in tumor DNA, D_{GAPDH} is the mean threshold cycle number for *GAPDH*

primer in tumor DNA, N_t is the mean threshold cycle number in reference DNA, and N_{GAPDH} is the mean threshold cycle number for *GAPDH* in reference DNA (modified from Le Bron et al. [33]).

Messenger RNA expression. Messenger RNA (mRNA) expression of selected candidate genes was also investigated by qRT-PCR, although the correlation between CNAs and mRNA expression is frequently affected by several confounding factors, including epigenetic alterations, such as methylation and miRNA expression [34], and large interindividual variation due to complex gene-gene regulation events [35]. RNA was isolated from frozen tissue samples using the RNeasy Lipid Tissue Minikit (Qiagen) and was reverse transcribed using the QuantiTect Reverse Transcription Kit (Qiagen). Predesigned TaqMan gene expression assays were purchased from Applied Biosystems (Darmstadt, Germany). Specific probes are given in the Table W1. Endogenously expressed β-actin was used as an internal control. Forty nanograms of cDNA was used for each PCR, and each sample was performed in duplicate. Transcript levels were determined by using the TaqMan Gene Expression Master Mix (Applied Biosystems), the C1000 Thermal Cycler (CFX96 real-time system; Biorad), and the Bio-Rad CFX Manager 2.0 software. Cycling conditions were 95°C for 3 minutes followed by 50 cycles of 95°C for 30 seconds, 60°C for 30 seconds, and 72°C for 30 seconds. Because of the small number of available matched normal adrenal tissues (area surrounding the adenomas), we could not design a threshold for altered expression based on the ratio between tumor and matched surrounding tissues. Using the ΔC_T method [36], the gene expression levels were normalized to those of the endogenous control β-actin, which was detected in all samples.

Results

Clinical Data

Our final study cohort included 15 tumor tissues and 15 matched blood samples from patients with cortisol-secreting ACA (10 women and 5 men; mean age at diagnosis, 47.5 ± 12.3 years). Eight patients had subclinical and seven had overt hypercortisolism. The mean diameter of the tumors was 4.2 ± 2.0 cm. Detailed clinical, pathologic, and corresponding genetic characteristics are provided in Table 1.

SNP Array Profiling Allowed the Identification of Recurrent CN Alterations in ACA

CN profiling revealed a total of 962 CNAs (564 gains and 398 losses). All cases were affected by at least two aberration with a median of 18 CNAs per sample (range, 2-284) showing a highly variable pattern (Table 1 and Figure 1). The chromosomes with the most frequent gains were chr 5, 3, 6, 11, and 2, whereas chromosomes with most frequent losses were chr 1, 6, and 2. The median length of CNAs was 29,071 bp (range, 587-7.71^{e7} bp). Large alterations (>100 kb) were rare events (11% of total), although they were found in most cases (12/15 adenomas; median per sample, 3; range, 0-82). CNAs longer than 10 Mb were observed in only 4/15 samples, involving the chromosomal regions 1p36.12-31.3 (loss), 1q21.1-23.1 and 1q24.2-31.2 (gain), 6q23.3-25.3 (loss) and 9q34.11-ter (gain), 17q11.2-25.3 (loss), 18p11.32-ter (loss), and 19p13.2-p12 (gain).

The list of all detected CNAs, including cytobands, type of alteration, length, number of markers, CN score, and overlapping genes according to the RefSeq database is provided in Table W2.

Several alterations were detected in intergenic regions, often localized at centromeric or telomeric segments (~50% of total CNAs). Thus, only 471 CNAs (198 gains and 273 losses; median per sample, 11; range, 0-197) were localized in regions with known genes.

Only 28% of all detected alterations were observed in at least two cases (i.e., minimal overlapping regions), indicating a high genetic variability among the samples. Considering only the aberrations found in regions coding for known genes, we observed 89 recurrent CNAs (51 gains and 38 losses) involving 73 chromosomal regions and 753 overlapping genes (Table W3). Among these, 18 gains had a CN score higher than 4.0, consistent with an amplification, and three losses had a CN score less than 1.0, which might be consistent with a homozygous deletion. However, no losses with a CN score less than 0.5 were observed that would clearly indicate a homozygous deletion.

In particular, 13 gains were recurrent in at least three cases (maximal frequency, ≥20%; median length, 1.85 Mb; Table W3). These alterations involved 11 chromosomal regions, 5 of them being in line with previous publication (Table 2). Intriguingly, most of them, namely gains in 5p15.33, 7p22.3-22.2, 8q24.3, 9q34.2-34.3, 11p15.5, 16q24.3, and Xq28, affected the same three ACAs (nos. 802A, 271A, and 207A)

Table 1. Summary of Clinical Features and Genetic Alterations Observed by the SNP Microarray Analysis (CNAs and cnLOH) of 15 Patients with Cortisol-Secreting ACA.

Patients	Sex/Age	Tumor Size (cm)	Hormonal Pattern*	Time of Follow-up (mo)	No. CNA (Gain/Loss)	No. cnLOH
1 (350A)	F/35	1.5	Subclinical	47	284 (30/254)	0
2 (802A)	F/55	6.5	Overt	29	237 (229/8)	0
3 (283A)	F/43	2.8	Subclinical	61	148 (148/0)	2
4 (312A)	M/71	11.0	Overt	60	123 (24/99)	1
5 (474A)	F/42	1.8	Overt	39	46 (46/0)	0
6 (170A)	M/53	5.0	Subclinical	151	34 (34/0)	3
7 (178A)	M/65	6.0	Subclinical	115	20 (4/16)	0
8 (207A)	F/41	3.0	Overt	99	18 (16/2)	0
9 (271A)	F/43	3.0	Overt	66	18 (13/5)	0
10 (967A)	F/29	3.3	Overt	14	13 (8/5)	0
11 (923A)	M/55	4.0	Subclinical	20	9 (6/3)	14
12 (223A)	F/45	NK	Overt	120	4 (1/3)	0
13 (1013A)	F/29	2.0	Subclinical	7	3 (2/1)	0
14 (226A)	M/47	2.5	Subclinical	82	3 (1/2)	0
15 (317A)	F/60	4.3	Subclinical	92	2 (2/0)	0
Mean	**47.5**	**4.0**		**66.8**	**64.1**	**1.4**
SD	**12.3**	**2.5**		**42.6**	**91.3**	**3.7**
Median	**45.0**	**3.2**		**61.0**	**18 (13/3)**	**0**

NK indicates not known.

*Overt or subclinical hypercortisolism according to previously described criteria [21].

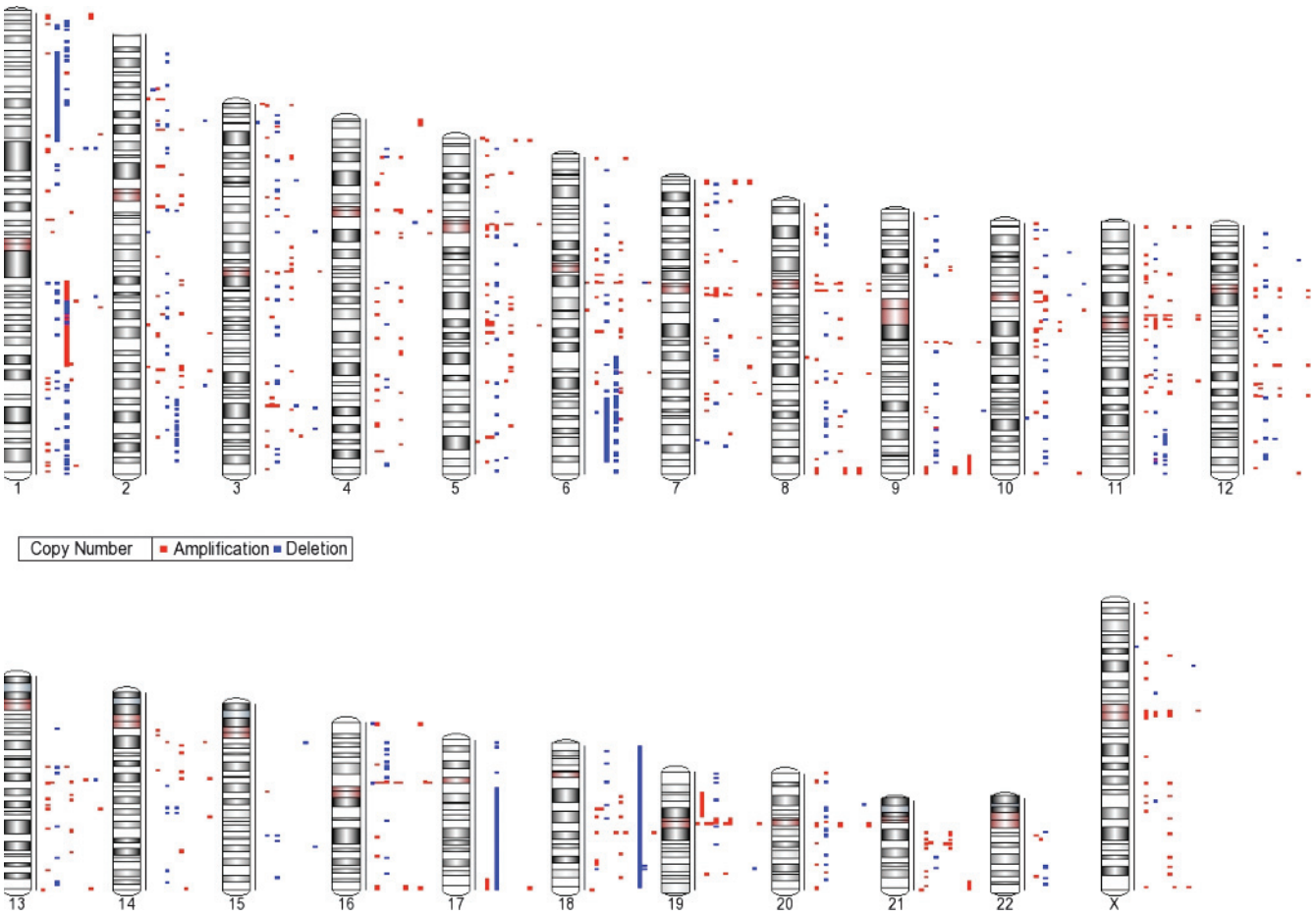

Figure 1. Genome-wide distribution of DNA CNAs in each cortisol-secreting adrenocortical benign tumor (n = 15). CN gains are represented in red and CN losses in blue.

associated with overt Cushing syndrome. Notably, potential candidate genes such as *NOTCH1*, *HRAS*, *IGF2*, *CYP2W1*, and *CYP11B2* are mapped in these regions.

The presence of the gain at 11p15.5 (*IGF2* locus) was also confirmed by FISH analysis in two of the three cases observed by SNP array (nos. 207A and 271A; data not shown).

Conversely, losses were all less than 1 Mb and occurred at most in two different samples. They were mostly localized in chr 1 (at 1p36.12-1p36.11, 1p34.2, 1p33, and 1q23.1), in chr 2 (at 2p16.2-16.1 and 2q11.2), at 3p22.1, at 6q21-26, in chr 11q (at 11q23.2 and 11q24.1-24.2), and in chr 18 (at 18p11.2-11.31 and 18q12.2) (Table W3).

Table 2. Chromosomal Regions with Most Frequent Gains (Minimal Overlapping Regions) Coding for Known Genes Observed in at Least 3/15 Cortisol-Secreting ACAs (Frequency, ≥20%) According to CNAs Detected by SNP Arrays.

Cytoband	Altered Samples	No. Genes	Selected Genes
Already reported regions*			
5p15.33	207A, 271A, 802A	28	*NKD2*, *PDCD6*
9q34.2-34.3	207A, 271A, 802A	100	*COBRA1*, *EDF1*, *FBXW5*, *LHX3*, *NOTCH1*, *RXRA*, *SNAPC4*, *TRAF2*
12q12		1	
16q24.3-	207A, 271A, 802A	14	*FANCA*, *MC1R*, *PRDM7*
20p11.1-q11.21	170A, 283A, 802A	3	
Newly observed regions			
6q16.1	283A, 474A, 802A	1	*EPHA7*
7p22.3-22.2	207A, 271A, 802A	34	*CYP2W1*, *MAFK*, *NUDT1*, *PDGFA*, *PRKAR1B*, *UNCX*
8q24.3	207A, 271A, 802A	102	*ARC*, *BAI1*, *SLURP1*, *ADCK5*, *CYP11B2*, *FOXH1*, *HSF1*, *LRRC14*, *MAFA*, *MAPK15*, *MFSD3*, *PUF60*, *RECQL4*
11p15.5	207A, 271A, 802A	74	*CD151*, *CTSD*, *H19*, *HRAS*, *IFITM1*, *IGF2*, *INS*, *INS-IGF2*, *IRF7*, *LRDD*, *PHRF1*, *RPLP2*, *SCT*
11q11	283A, 350A, 802A	3	
Xq28	207A, 271A, 802A	81	*DKC1*, *IRAK1*, *L1CAM*, *MECP2*

Selected genes: genes considered relevant for tumorigenesis or glucocorticoid production/effects. They include potential oncogenes and tumor suppressor genes, growth or transcription factors, cell differentiation markers, protein kinases (according to the gene set enrichment analysis, see also Table W4), genes involved in steroidogenesis (underlined), or glucocorticoid regulation or in Wnt/β-catenin signaling.

Localization, length, and CN score of the CNAs are reported in Table W3.

*Regions already reported in previous studies with conventional comparative genomic hybridization [3,12,13].

ACA Are Affected by Recurrent Microalterations

The extremely high-resolution allowed us to identify 309 CN microalterations (127 gains and 182 losses, 66% of CNAs in regions coding for known genes) that involved 285 single genes (including 60 introns). Some of these microalterations affected only specific structural regions of single genes.

Forty-six of these small alterations occurred in two or more cases (18 gains, 13 amplifications, and 15 losses; Table 3). A representative example of recurrent microamplification at the *ephrin receptor 7* (*EPHA7*) gene is shown in Figure 2. With the exception of a gain in 10p11.21, none of these microalterations have been reported previously in human tissue samples from healthy subjects (according to the dBVar).

The presence of the microdeletion at 6q23.2 (locus for *SGK1*) in sample 350 was confirmed also by FISH analysis showing a locus-specific loss for *SGK1* in more than 80% of the cells (Figure 3). Because no paraffin block from the other tumor affected by a loss of *SGK1* locus (no. 312A) was available, no confirmation by FISH was possible.

ACA Are Affected by cnLOH

We identified 23 LOH events in 12 regions on chr 1, 7, 9, 11, and 16, involving 5/15 adenomas. The median length of these alterations was 69,420 bp (range, 1,526-4,495,281 bp). None of the regions with LOH were also affected by a CN loss, suggesting that all the LOH occurred along with a gain of the remaining chromosomal copy. Specifically, three LOHs were associated with a gain (at 1q23.3 and 9q31.2), whereas 20 were cnLOH events (Table 4). cnLOH events were observed in 4 different adenomas (26.6%) and distributed on 11 chromosomal regions with a median size of 108,415 bp (range, 25,701-3,445,898 bp), 16q being the most frequently altered regions. Overall, 15 known genes were affected, including the potential tumor

Table 3. Most Frequent Microalterations Involving Single Genes in 15 Cortisol-Secreting ACAs According to CNAs Detected by High-resolution SNP Arrays.

Cytoband	*n* (%)	CNA	CN Score	Gene	Description
12q12	3 (20)	Gain	5.23	Contained within *C12orf40*	Chromosome 12 open reading frame 40
6q16.1	3 (20)	Gain	4.33	Contained within ***EPHA7***	Ephrin receptor 7
9q34.3	3 (20)	Gain	3.64	Overlap with 51% of *FAM157B*	Family with sequence similarity 157, member B
2q11.2	2 (13)	Gain	4.71	Intron of *C2orf55*	Chromosome 2 open reading frame 55
Xq22.3	2 (13)	Gain	4.60	Contained within *IL1RAPL2*	Interleukin 1 receptor accessory protein-like 2
11q14.1	2 (13)	Gain	4.57	Intron of *DLG2*	Discs large homolog 2
12q21.31	2 (13)	Gain	4.51	Intron of *MGAT4C*	Mannosyl-glycoprotein β-1,4-*N*-acetylglucosaminyltransferase, isozyme C
2q24.3	2 (13)	Gain	4.36	Contained within *SCN9A*	Sodium channel, voltage-gated, type IX, α subunit
12q21.32	2 (13)	Gain	4.27	Intron of ***KITLG***	KIT ligand
14q21.3	2 (13)	Gain	4.26	Contained within *MDGA2*	MAM domain containing glycosylphosphatidylinositol anchor 2
12q13.3	2 (13)	Gain	4.02	*TAC3*	Tachykinin 3
4p15.31	2 (13)	Gain	4.00	Intron of *KCNIP4*	Kv channel interacting protein 4
3p14.2	2 (13)	Gain	3.95	Intron of ***FHIT***	Fragile histidine triad gene
10q11.21	2 (13)	Gain	3.92	Overlap with 54% of *ZNF33B*	Zinc finger protein 33B
10p11.21	2 (13)	Gain	3.91	Contained within *ANKRD30A*	Ankyrin repeat domain 30A
2p12	2 (13)	Gain	3.85	Intron of *LRRTM4*	Leucine-rich repeat transmembrane neuronal 4
10q21.1	2 (13)	Gain	3.81	Intron of ***PRKG1***	Protein kinase, cGMP-dependent, type I
13q14.2	2 (13)	Gain	3.79	Intron of *CAB39L*	Calcium binding protein 39-like
1q44	2 (13)	Gain	3.68	Intron of *KIF26B*	Kinesin family member 26B
18q12.3	2 (13)	Gain	3.49	Intron of *RIT2*	Ras-like without CAAX 2
11p11.12	2 (13)	Gain	3.34	*OR4A5*	Olfactory receptor family 4 subfamily A member 5
7p13	2 (13)	Gain	3.10	Contained within ***CAMK2B***	Calcium/calmodulin-dependent protein kinase II β
Xq28	2 (13)	Gain	2.91	Overlap with 88% of *IDH3G*	Isocitrate dehydrogenase [NAD] subunit gamma, mitochondrial precursor
Xq28	2 (13)	Gain	2.83	Intron of *F8*	Coagulation factor VIII precursor
7p22.2	2 (13)	Gain	2.73	Intron of *GNA12*	G protein alpha 12
8q24.3	2 (13)	Gain	2.64	***CYP11B1***	Cytochrome P450 11B1, mitochondrial precursor
8q24.3	2 (13)	Gain	2.64	*C8orf33*	Chromosome 8 open reading frame 33
5p15.33	2 (13)	Gain	2.61	***IRX4***	Iroquois homeobox 4
6q23.2	2 (13)	Loss	0.84	Contained within ***SGK1***	Serum/glucocorticoid-regulated kinase 1
2q11.2	2 (13)	Loss	0.88	Intron of ***NPAS2***	Neuronal PAS domain protein 2
3p22.1	2 (13)	Loss	0.96	Contained within ***CTNNB1***	Catenin (cadherin-associated protein), β 1
6q22.31	2 (13)	Loss	1.00	***HEY2***	Hairy/enhancer-of-split related with YRPW motif 2
6q26	2 (13)	Loss	1.01	Contained within *QKI*	Quackin protein
18q11.2	2 (13)	Loss	1.10	Contained within *LAMA3*	Laminin subunit alpha-3 precursor
6q21	2 (13)	Loss	1.02	Overlap with 70% of ***REV3L***	DNA polymerase zeta catalytic subunit
2p16.2-.1	2 (13)	Loss	1.03	Overlap with 50% of *EML6*	Echinoderm microtubule-associated protein like 6
1q23.1	2 (13)	Loss	1.12	*CD5L*	CD5 antigen-like precursor
6q23.3	2 (13)	Loss	1.13	Contained within *KIAA1244*	
1p36.11	2 (13)	Loss	1.16	Overlap with 60% of *TMEM57*	Macoilin (transmembrane protein 57)
11q23.2	2 (13)	Loss	1.16	*FAM55D*	Family with sequence similarity 55, member D
18q12.2	2 (13)	Loss	1.18	Intron of *FHOD3*	FH1/FH2 domain-containing protein 3
6q23.1	2 (13)	Loss	1.29	Contained within *EPB41L2*	Erythrocyte membrane band 4.1-like protein 2
6q25.2	2 (13)	Loss	1.31	Overlap with 81% of *RGS17*	Regulator of G protein signaling 17
1p33	2 (13)	Loss	1.34	***STIL***	SCL-interrupting locus protein
6q26	2 (13)	Loss	1.35	Intron of *PACRG*	PARK2 coregulated
6q25.1-.2	2 (13)	Loss	1.36	Overlap with 80% of *SYNE1*	Synaptic nuclear envelope protein 1

Only CNAs involving one entire gene or contained within one gene or overlapping with more than 50% of one gene are reported.
Genes in **bold**: genes considered relevant for tumorigenesis or glucocorticoid production/effects. They include potential oncogenes and tumor suppressor genes, growth or transcription factors, cell differentiation markers, protein kinases (according to GSEA; see also Table W4), genes involved in steroidogenesis (underlined) or glucocorticoid regulation or in Wnt/β-catenin signaling.

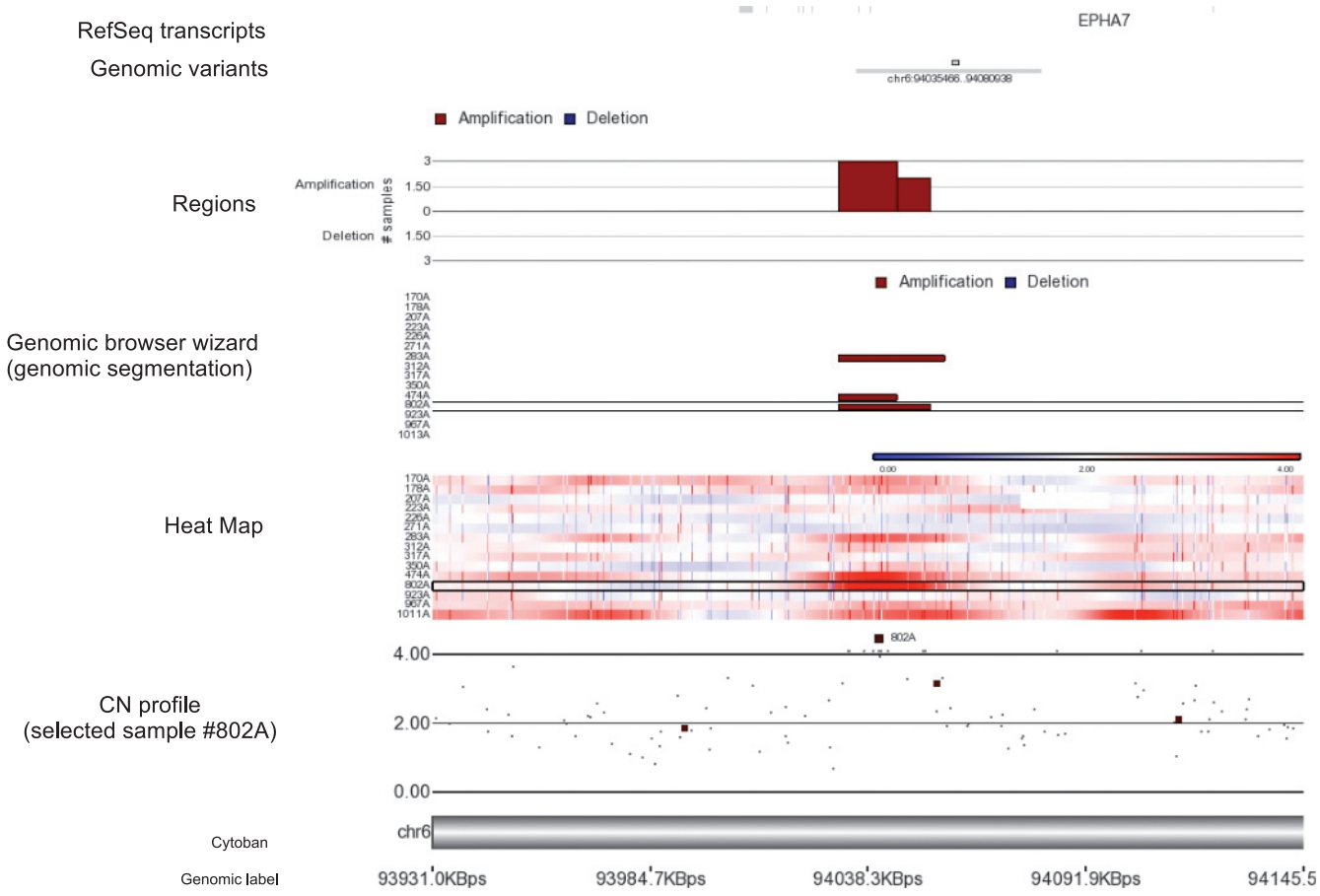

Figure 2. A representative example of a single gene (ephrin receptor 7 [*EPHA7*] at chr 6q16.1; entire length, 179,563 bp) affected by a recurrent SNP-detected microamplification. The heat map shows the intensity plots in each sample (defined with sample ID). Gains/amplifications are represented in red and losses/deletions in blue. The CN profile is shown for three altered cases (nos. 283A, 474A, 802A). The genomic browser wizard shows the altered regions (gains represented in red and losses in blue) according to the genomic segmentation (Partek GS). Minimal overlapping regions in at least 2 samples (MORs) are reported in the upper panel (length of the MOR, 14,544 bp).

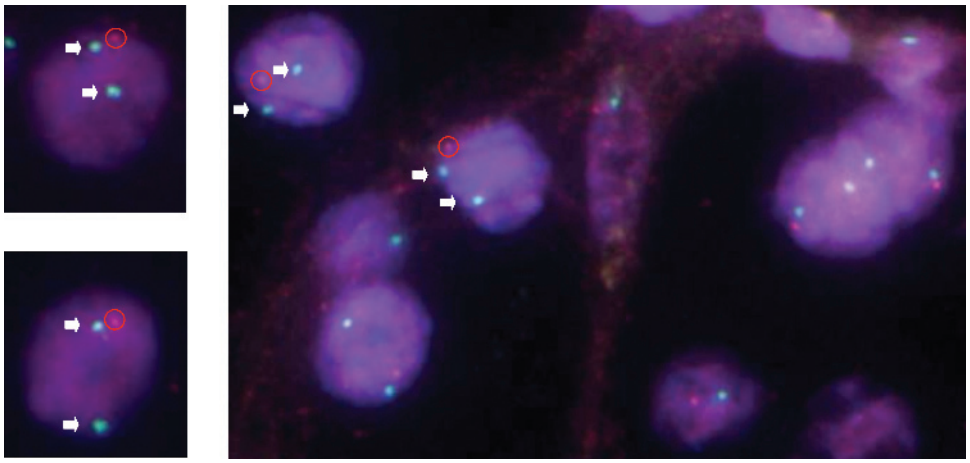

Figure 3. Validation with FISH analysis of the CNAs detected with SNP array. Representative FISH-validated case with CN loss at the *SGK1* locus (probe at 6q23.2) according to the SNP analysis (sample no. 350A): loss of the red signal (specific for the SGK1 probe) with respect to the green signal (centromere-specific reference probe) in more than 80% of cells. Arrows indicate the additional green signals, whereas red circles underline the red signals.

Table 4. LOH Events Detected by High-resolution SNP Arrays in 15 Cortisol-Secreting ACAs.

Cytoband	No. LOH	Type of Alteration	Length (bp)	Altered Sample	HR	Overlapping Genes
1p33	1	cnLOH	25,701	312A	0.17	Region overlaps with 90% of *CMPK1*
1q23.3	2	LOH + gain	61,241	312A	0	Intron of *PBX1*
7q11.21	2	cnLOH	108,415	283A	0	*LOC643955*
9q31.2	1	LOH + gain	6,944	802A	0	Not coding
11p11.12-11q11	2	cnLOH	3,445,898	170A	0.012	*OR4C46*
11q11	1	cnLOH	74,179	170A	0.012	*TRIM48*
16q12.1	1	cnLOH	215,106	923A	0.14	*ADCY7*, *BRD7*
12.2	3		58,676		0.077	Intron of *FTO*, region overlaps with 70% of *RPGRIP1L*
16q21-22.1	4	cnLOH	111,178	923A	0.018	*CKLF*, *CMTM1*, *CMTM2*, *TK2*
16q23.1	3	cnLOH	336,158	923A	0.021	Region overlaps with 62% of *CNTNAP4*, region overlaps with 60% of *VAT1*
23.2	1		47,149		0.067	Not coding
16q24.1	1	cnLOH	11,758	923A	0	Not coding
24.2	1		25,499		0.095	Region overlaps with 83% of *ZCCHC14*

BRD7 indicates potential tumor suppressor gene; HR, heterozygous rate.

suppressor gene *bromodomain containing 7* (*BRD7*) mapped at 16q12.1 (Table 4).

Correlation between CNA and Clinical Features

Tumor size positively correlated with the number of large CNAs (>100 kb, $P = .042$, $r = 0.28$). This was even more evident when only large losses were considered ($P = .039$, $r = 0.56$). Cortisol levels after DST correlated with the number of large gains. However, this correlation was not significant. In addition, all the three adenomas that were affected by the most common large CN gains (nos. 802A, 207A, and 271A) had an overt hypercortisolism.

No significant correlations between the total number of detected CNAs and/or cnLOH and the clinical parameters, such as sex, age at diagnosis, tumor size, hormonal hypersecretion, body mass index, blood pressure, and duration of follow-up, were found in our series. Moreover, no differences were observed between different subgroups of patients regarding tumor size or severity of hypercortisolism.

Identification of Candidate Genes

We analyzed all the 753 genes with CN gains or losses in at least two cases (listed in Table W3) and 638 known overlapping genes were recognized in Gene Ontology (572 gained and 66 lost). Interestingly, among the genes with CN gains, 19 microRNAs (including MIR483, MIR126, and MIR675), three small nucleolar RNA and two noncoding RNA have also been recognized (Table W3).

Using the GSEA tool, the annotation to gene families showed several transcription factors ($n = 48$) and protein kinases ($n = 15$), especially among the genes with CN gains (Table W4).

The MetaCore analysis was also applied on these 753 genes to examine their association with known canonical pathways (GeneGO Pathways Maps). The most significant recognized pathway was the Notch signaling ($P = 1.494^{e-6}$). It was followed by the Wnt and Notch signaling in early cardiac myogenesis ($P = 4.287^{e-6}$) and in osteogenesis ($P = 1.094^{e-5}$), by the reverse signaling by Ephrin B, which also includes the Wnt/β-catenin pathway ($P = 2.549^{e-5}$) and the WNT5A signaling pathway ($P = 2.764^{e-5}$). The first two most significant pathways and their associated genes are shown in the Figure W2, *A* and *B*, whereas the entire Notch signaling gene network and its known connections with the Wnt/β-catenin signaling pathway is shown in Figure W3 (GeneGO).

According to the global STRING-generated protein-protein network including the same group of genes, we observed that *CTNNB1* and *INS/IGF2* were among the most central molecules (data not shown).

Among the 285 annotated genes affected by chromosomal microamplifications, we recognized protein kinases (such as *CAMK2B*, *EPHA7*, *PRKG1*), the growth factor *KITLG*, the tumor suppressor gene *FHIT*, the suggested transforming oncogene *GNA12*, the steroid 11-β-hydroxylase *CYP11B1*, and ion channels (such as *SCN9A* and *KCNIP4*), as particular interesting; whereas among genes affected by microdeletions, we recognized transcription factors, such as *HEY2*, *NPAS2*, and *REV3L*, the protein kinase *SGK1*, and the oncogenes *CTNNB1* and *STIL* (Tables 3, W3, and W4).

By STRING analysis including only genes with microalterations recurrent in at least two samples ($n = 46$), the most central interactions were observed between *CTNNB1* and *FHIT*, *SGK1*, and *KITLG* (Figure W4).

The validation with qRT-PCR at the DNA level for single altered genes showed a reasonable fit for *SGK1* (75% correspondence), *CTNNB1* and *EPHA7* (64% correspondence). Most discrepancies to SNP arrays results were observed in alterations with CN scores close to the cutoff level (Figure 4*A*).

mRNA Expression of Candidate Genes

The mRNA expression levels of selected candidate genes from amplified (*IGF2*, *EPHA7*, *CYP11B1*, *CYP11B2*, *NOTCH1*, *HRAS*, and *FHIT*) and deleted areas (*SGK1* and *CTNNB1*) were analyzed by qRT-PCR. Owing to the small number of detected CNA, a statistical comparison between SNP results and gene expression was not feasible. However, interestingly, the chromosomal gains within the *CYP11B1* locus and the losses within the *SGK1* locus showed an association with an increase and a decrease in mRNA expression levels, respectively (Figure 4*B*).

Discussion

We here provide for the first time a genome-wide and high-resolution view of chromosomal changes in benign adrenocortical tumors, based on SNP arrays 6.0 covering simultaneously CNA and LOH. Previous studies have established SNP arrays as a powerful tool to detect DNA changes in solid tumors, revealing loci and candidate genes possibly involved in tumorigenesis [22–24]. To reduce the influence of disease

heterogeneity and false-positives, we focused on cortisol-secreting ACAs using a paired analysis approach with corresponding blood samples and a stringent mathematical algorithm. This method allowed us to identify novel chromosomal regions affected by CNA and novel promising candidate genes. Moreover, we were able to recognize among the altered genes, several members of signaling pathways that, until now, have not been associated with adrenocortical tumorigenesis.

CNAs were invariably observed in all our cases with a rather high median number of CNAs per sample. In contrast, previous cytogenetic studies applying CGH on benign adrenocortical tumors had revealed only few gains or losses [14–16,18,19]. This discrepancy reflects the much higher resolution of the Affymetrix SNP 6.0 array platform (estimated resolution limit of 7 kb) compared with CGH (10 Mb for conventional CGH and of 150 kb for array CGH). Accordingly, most of the detected CNAs were microalterations (89% of total). However, consistent with previous findings [14,16–18], we found a high variability of the number of CNAs among different samples and a significant correlation with the tumor size when considering only the longer alterations (>100 kb).

Recurrent CN Gains and Candidate Genes

We observed frequent CN gains (≥20% of cases) in already reported regions, confirming the reliability of our SNP array analysis but also in not-yet-described regions (Table 2). In all these regions, we identified

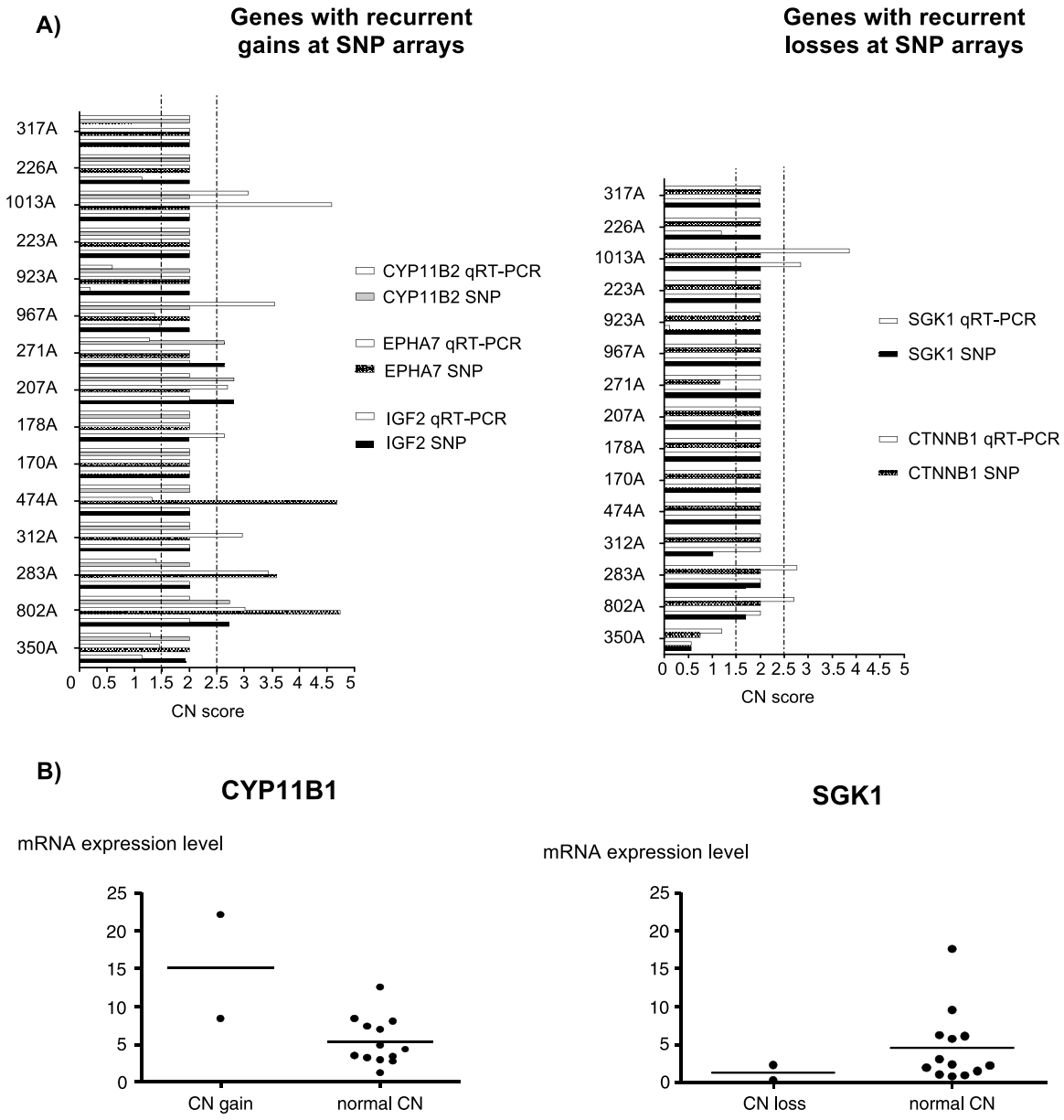

Figure 4. (A) Validation of CNAs detected with SNP array. CNA analysis by qRT-PCR at the DNA level for five selected candidate genes with gains (*CYP11B2*, *EPHA7*, *IGF2*) or losses (*CTNNB1*, *SGK1*) according to the SNP array analysis. CN score of 2 corresponds to normal CN; CN score greater than 2.5, CN gain; CN score less than 1.5, CN loss. The best fit was observed for the genes *SGK1* (75% correspondence), *CTNNB1* and *EPHA7* (64% correspondence). (B) Relative mRNA expression levels evaluated by qRT-PCR for two selected candidate genes (*CYP11B1* and *SGK1*) according to the CN status observed with SNP array analysis. The gene actin beta was used as a loading control (reference gene).

candidate genes, which have not been implicated in adrenal tumorigenesis so far. In particular, we were able to confirm gains at chr 5, 9q (telomeric region), 12q, and chr 16 [14–16,18], and interestingly, we could narrow down these regions to smaller segments such as 5p15.33, 9q34.2-34.3, 12q12, and 16q24.3-tel.

Notably, we did not recognize at 9q34 alterations in the *NR5A1* gene coding for the steroidogenic factor (SF-1), which is involved in the regulation of steroid biosynthesis and is a marker to differentiate between tumors of adrenocortical and nonadrenocortical origin [37]. Similar results have been obtained with SNP array profiling in childhood adrenocortical tumors (E. Lalli, personal communication), maybe suggesting that other mechanisms may account to SF1 overexpression and/or that other genes in this region may play an important pathogenetic role. In fact, the 9q34 region comprised among others the *NOTCH1* gene, which plays a role in a variety of developmental processes and tumorigenesis by controlling cell fate decisions. In particular, Notch1 may either suppress or promote tumor development and progression depending on cell type and context [38]. For instance, Notch1 is inactive in several neuroendocrine malignancies, including medullary thyroid cancer, carcinoid, and small cell lung cancer.

Among the newly observed regions with gains, the 11p15.5 imprinted locus, which comprises several genes like *IGF2*, *INS*, *INS-IGF2*, and *H19*, is of particular interest. It is well known that in ACC paternal isodisomy in this locus (cnLOH) leads to IGF2 overexpression, which is correlated with malignancy [39]. On the basis of our findings, it could be hypothesized that a gain of the paternal allele in this region acts as a "first hit" in the development of ACC. The loss of the maternal allele might then act as a "second hit" (cnLOH), leading to IGF2 overexpression and malignant progression. Thus, these observations could be a hint toward a stepwise progression from a benign to a malignant phenotype in adrenal tumorigenesis. Moreover, the well-known oncogene *HRAS*, which was previously found to be occasionally mutated in ACC [40] and which might play a supporting role in tumor progression, is also included among gained genes at 11p15.5.

Notably, among the altered genes mapped in many of the recurrently gained regions (i.e., at 7p22.3-22.2, 8q24.3, 9q34.2-34.3, 11p15.5, 1p36.3-36.2, 10q26.3, and 16p13.3), we recognized several microRNAs that could theoretically regulate gene expression. In particular, they included the MIR483 and MIR675, which have already been reported to be altered in adrenocortical tumors [41,42].

Even more interestingly, most of the recurrent gains were identified in the same three ACAs that all had an overt hypercortisolism (20% of all patients, 43% of patients with overt hypercortisolism). Specifically, they were localized in seven different chromosomes (namely at 5p15.33, 7p22.3-22.2, 8q24.3, 9q34.2-34.3, 11p15.5, 16q24.3, and Xq28). It could be hypothesized that these recurrent alterations could affect early adrenocortical tumorigenesis and/or on corticosteroid overproduction. Accordingly, several pathophysiologically relevant genes, including the known oncogenes *NOTCH1* and *HRAS*, the *IGF2*, involved in adrenocortical tumor development, and the aldosterone-synthase *CYP11B2* were located in these regions. Moreover, two of these three ACAs had also an additional microamplification in the gene coding for the 11-β-hydroxylase (*CYP11B1*), which was also somehow correlated with a high mRNA expression. Nevertheless, the gains found at *CYP11B2* were not associated with both mRNA expression and clinical data. These findings further suggest a possible role of CN gains in genes coding for enzymes involved in steroidogenesis on hormonal hypersecretion pathogenesis.

Recurrent Microalterations and Candidate Genes

One of the most striking finding was the observation that many CNAs affected only single genes (Table 3), which represent a major advantage of this study compared with previous investigations using CGH. The most frequent microamplification (n = 3) was detected in the gene *EPHA7*, which was confirmed in two cases by DNA qRT-PCR. The ephrin receptors represent the largest family of receptor tyrosine kinases. They are frequently overexpressed in a wide variety of cancer types, but they can be downregulated in advanced tumor stages [43], thus representing potential promising therapeutic targets in cancer. We observed gains contained in *EPHA7* in three adenomas, and additional single cases had gains in *EPHA6*, *EPHB3* or *EPHB4* or losses in *EPHA6*, *EPHA8*, or *EPHB2*, suggesting a role of the ephrin receptor family in adrenocortical tumorigenesis, which needs further investigation.

We also observed, among others, microdeletions in the genes *CTNNB1* and *SGK1* (frequency, ≥13%), whose central role among other associations was supported by the STRING analysis. Constitutive activating mutations in *CTNNB1* are known to be frequent in adrenocortical tumors, usually leading to a β-catenin accumulation in the cytoplasm and translocation to the nucleus, and are found to correlate with poor prognosis in ACC and hormonal inactivity [11]. Nevertheless, somatic *CTNNB1* mutations may explain only approximately 50% of the β-catenin accumulation, indicating that other components of the Wnt pathway may be involved [44]. No data about CNAs or other genetic changes in CTNNB1 existed so far, and the effective role of a CN loss in benign tumors remains to be better characterized.

SGK1 is a ubiquitously expressed serine/threonine kinase originally cloned as a glucocorticoid early-response gene. Its expression is upregulated by a number of other factors including β-catenin [11,45] and is activated by p53 [46]. SGK1 is a downstream effector of phosphatidylinositide-3-kinase and is involved in several biologic functions, including cell survival, and may be involved in resistance to chemotherapy [47]. However, its definitive role on tumor growth is still conflicting, as its expression is upregulated in some tumors and downregulated in others. SGK1 expression and function have been recently investigated in corticotroph cell lines [48], in response to corticosterone elevation induced by stress in mice [49] and in several cancers [50], but its role in adrenocortical tumors and/or endogenous hypecortisolism is unknown. CN losses in *SGK1* gene were also confirmed by FISH and DNA qRT-PCR analysis and corresponded to a low mRNA expression level.

cnLOH and Candidate Genes

Another relevant advantage of SNP arrays is the possibility to also detect cnLOH (or UPD). Accordingly, the number of UPD cases reported in the literature has recently increased exponentially and recurrent cnLOHs have been reported in many cancer types, possibly constituting an important driving force in cancer [51]. In fact, it has been shown that neoplastic cells not only depend on structural alterations of genetic material but also on the presence of cnLOH, which may produce homozygosity for a preexisting tumor somatic mutation [27]. In our series, we detected only a few small cnLOH, none of them being observed in more than one sample, likely because of the benign nature of our tumors. However, some interesting genes were mapped into regions of cnLOH, such as *BRD7*, a potential tumor suppressor gene acting as a transcriptional cofactor for p53. The potential pathogenetic role of these alterations remains to be elucidated.

Candidate Signaling Pathways

According to a pathway analysis including the 753 genes altered in at least two cases, the Notch1 and the Wnt/β-catenin signaling were the most significantly affected pathways. In fact, we observed CN gains or losses in several genes involved in different steps of the Notch1 (i.e., namely *p73*, *NOTCH1*, *HES4*, *HES5*, *HEY2*, *CTNNB1*) and/or the Wnt/β-catenin pathway (i.e., *LRP5*, *DVL1*, *AXIN1*, *NKD2*, *CTNNB1*, *SGK1*), which are closely interconnected. On one hand, a constitutive activation of the Wnt/β-catenin signaling pathway is well known to be common in adrenocortical tumors, but the underlying molecular mechanism is only partially elucidated [11–13]. Nevertheless, an aberrant Notch signaling has been linked to a wide variety of tumors such as small cell lung cancer, neuroblastoma, cervical, and prostate cancer, but it has not been yet implicated in adrenocortical neoplasias. In addition, it is known that the Notch1 and the Wnt/β-catenin pathways interact in different contexts and comprise genes that regulate each other transcriptionally [52]. For instance, activation of Notch signaling is β-catenin dependent in melanoma progression [53], whereas an antioncogenic effect seemed to be mediated by p21 induction and Wnt signaling repression in skin carcinogenesis. In this context, as shown in the Figure 5, a relevant role might be also suggested for other factors, such as SGK1, which is also a target gene of β-catenin. In fact, stimulation of SGK1 by glucocorticoids, in combination with activated PKB/Akt complex, phosphorylates glycogen-synthase-kinase-3 to inactivate this kinase, thus inhibiting β-catenin degradation in the proteasome and producing a stabilized hypophosphorylated form of β-catenin [54]. It has also been demonstrated that SGK1 negatively controls Notch1 protein expression and transcriptional activity by modulating intracellular Notch1 stability through Fbw7 phosphorylation [55]. Our findings obtained with pathway analysis reveal a novel potential role of Notch signaling pathway disruption and a possible key connection with Wnt/β-catenin signaling in early adrenocortical tumorigenesis. A further confirmation of the supposed Notch1 signaling pathway activation (i.e., through the investigation of the specific target genes) and a more detailed understanding of its potential molecular interactions may provide a framework for future therapies targeting these pathways and downstream genes.

In summary, our findings provide the first high-resolution genome-wide view of genomic changes in benign adrenocortical cortisol-secreting tumors, revealing recurrent gains and losses in novel chromosomal

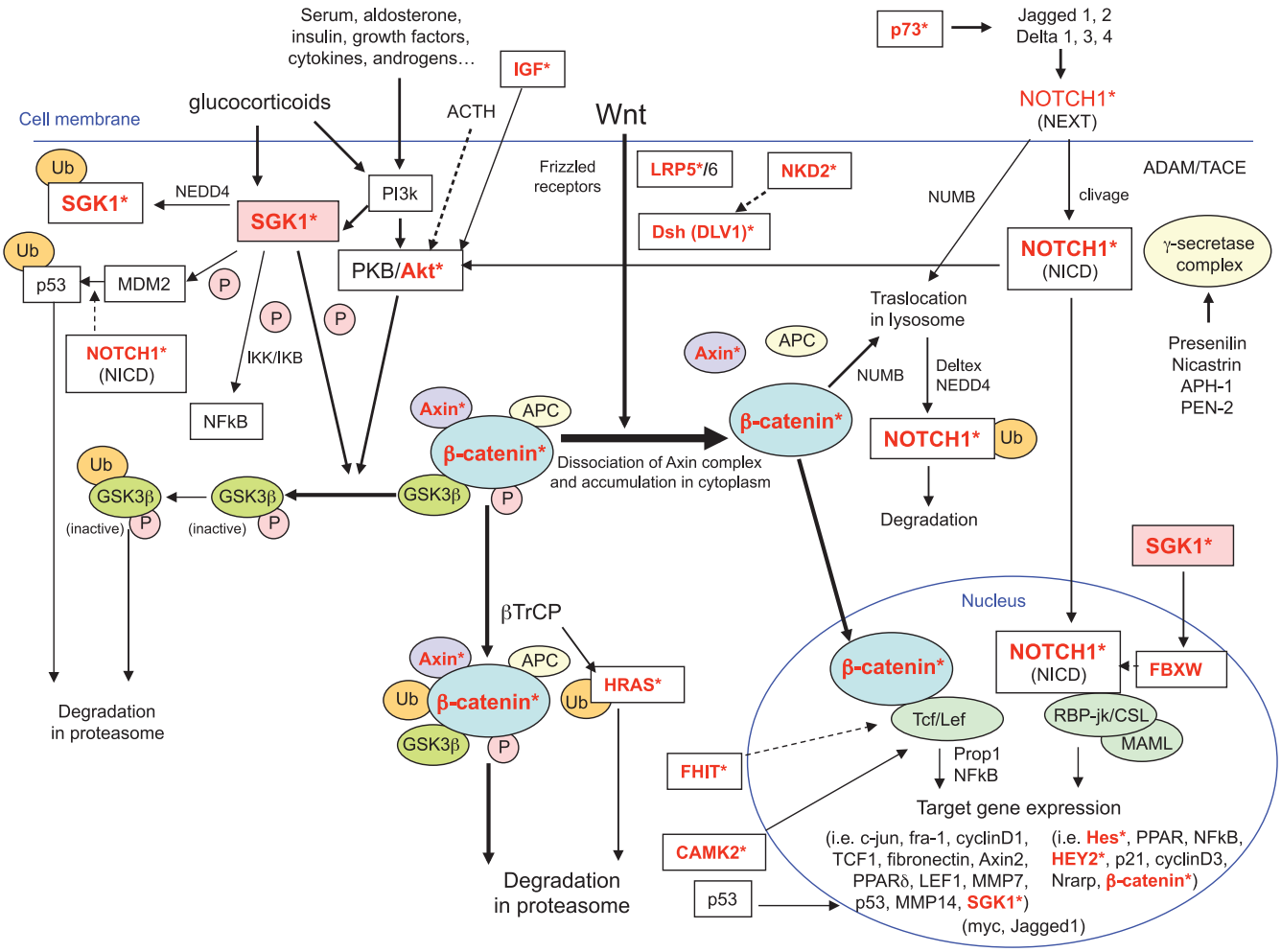

Figure 5. Graphical representation of the known connections between the Wnt/β-catenin pathway and the Notch1 signaling pathways, according to the knowledge of the current literature. Additional factors, such as SGK1, are also reported. Sources are represented by previous articles [11,46–49]. Genes with CNAs according to the SNP array analysis (gains or losses) in at least two samples from our series of 15 cortisol-secreting ACAs (frequency, ≥13%) are reported in red with an asterisk. NEXT indicates Notch extracellular domain; NICD, Notch intracellular domain.

regions and identifying new candidate genes, such as *HRAS*, *EPHA7*, and *SGK1*, which might be involved in early tumorigenesis. Furthermore, our results suggest a potential important role of the Notch1 signaling and its connections with the Wnt/β-catenin signaling pathway in the molecular pathogenesis of benign cortisol-secreting tumors.

Acknowledgments

The authors thank the technical assistants for expert and kind help, including Luitgard Kraus for DNA extraction, Sonja Steinhauer for RNA extraction and cDNA transcription, and Theodora Nedeva for SNP microarray and FISH analysis performance.

References

[1] Mansmann G, Lau J, Balk E, Rothberg M, Miyachi Y, and Bornstein SR (2004). The clinically inapparent adrenal mass: update in diagnosis and management. *Endocr Rev* **25**, 309–340.

[2] Fassnacht M, Libe R, Kroiss M, and Allolio B (2011). Adrenocortical carcinoma: a clinician's update. *Nat Rev Endocrinol* **7**, 323–335.

[3] Bernard MH, Sidhu S, Berger N, Peix JL, Marsh DJ, Robinson BG, Gaston V, Le Bouc Y, and Gicquel C (2003). A case report in favor of a multistep adrenocortical tumorigenesis. *J Clin Endocrinol Metab* **88**, 998–1001.

[4] Barzon L, Sonino N, Fallo F, Palu G, and Boscaro M (2003). Prevalence and natural history of adrenal incidentalomas. *Eur J Endocrinol* **149**, 273–285.

[5] Bassett MH, Mayhew B, Rehman K, White PC, Mantero F, Arnaldi G, Stewart PM, Bujalska I, and Rainey WE (2005). Expression profiles for steroidogenic enzymes in adrenocortical disease. *J Clin Endocrinol Metab* **90**, 5446–5455.

[6] Lindholm J, Juul S, Jorgensen JO, Astrup J, Bjerre P, Feldt-Rasmussen U, Hagen C, Jorgensen J, Kosteljanetz M, Kristensen L, et al. (2001). Incidence and late prognosis of Cushing's syndrome: a population-based study. *J Clin Endocrinol Metab* **86**, 117–123.

[7] Ragazzon B, Assie G, and Bertherat J (2011). Transcriptome analysis of adrenocortical cancers: from molecular classification to the identification of new treatments. *Endocr Relat Cancer* **18**, R15–R27.

[8] Stratakis CA (2009). New genes and/or molecular pathways associated with adrenal hyperplasias and related adrenocortical tumors. *Mol Cell Endocrinol* **300**, 152–157.

[9] Sidhu S, Gicquel C, Bambach CP, Campbell P, Magarey C, Robinson BG, and Delbridge LW (2003). Clinical and molecular aspects of adrenocortical tumourigenesis. *ANZ J Surg* **73**, 727–738.

[10] Gicquel C, Bertagna X, Gaston V, Coste J, Louvel A, Baudin E, Bertherat J, Chapuis Y, Duclos JM, Schlumberger M, et al. (2001). Molecular markers and long-term recurrences in a large cohort of patients with sporadic adrenocortical tumors. *Cancer Res* **61**, 6762–6767.

[11] Bonnet S, Gaujoux S, Launay P, Baudry C, Chokri I, Ragazzon B, Libe R, Rene-Corail F, Audebourg A, Vacher-Lavenu MC, et al. (2011). Wnt/β-catenin pathway activation in adrenocortical adenomas is frequently due to somatic CTNNB1-activating mutations, which are associated with larger and nonsecreting tumors: a study in cortisol-secreting and -nonsecreting tumors. *J Clin Endocrinol Metab* **96**, E419–E426.

[12] Gaujoux S, Grabar S, Fassnacht M, Ragazzon B, Launay P, Libe R, Chokri I, Audebourg A, Royer B, Sbiera S, et al. (2011). β-Catenin activation is associated with specific clinical and pathologic characteristics and a poor outcome in adrenocortical carcinoma. *Clin Cancer Res* **17**, 328–336.

[13] Tadjine M, Lampron A, Ouadi L, and Bourdeau I (2008). Frequent mutations of β-catenin gene in sporadic secreting adrenocortical adenomas. *Clin Endocrinol (Oxf)* **68**, 264–270.

[14] Dohna M, Reincke M, Mincheva A, Allolio B, Solinas-Toldo S, and Lichter P (2000). Adrenocortical carcinoma is characterized by a high frequency of chromosomal gains and high-level amplifications. *Genes Chromosomes Cancer* **28**, 145–152.

[15] Sidhu S, Marsh DJ, Theodosopoulos G, Philips J, Bambach CP, Campbell P, Magarey CJ, Russell CF, Schulte KM, Roher HD, et al. (2002). Comparative genomic hybridization analysis of adrenocortical tumors. *J Clin Endocrinol Metab* **87**, 3467–3474.

[16] Zhao J, Speel EJ, Muletta-Feurer S, Rutimann K, Saremaslani P, Roth J, Heitz PU, and Komminoth P (1999). Analysis of genomic alterations in sporadic adrenocortical lesions. Gain of chromosome 17 is an early event in adrenocortical tumorigenesis. *Am J Pathol* **155**, 1039–1045.

[17] Gruschwitz T, Breza J, Wunderlich H, and Junker K (2010). Improvement of histopathological classification of adrenal gland tumors by genetic differentiation. *World J Urol* **28**, 329–334.

[18] Kjellman M, Kallioniemi OP, Karhu R, Hoog A, Farnebo LO, Auer G, Larsson C, and Backdahl M (1996). Genetic aberrations in adrenocortical tumors detected using comparative genomic hybridization correlate with tumor size and malignancy. *Cancer Res* **56**, 4219–4223.

[19] Zhao J, Roth J, Bode-Lesniewska B, Pfaltz M, Heitz PU, and Komminoth P (2002). Combined comparative genomic hybridization and genomic microarray for detection of gene amplifications in pulmonary artery intimal sarcomas and adrenocortical tumors. *Genes Chromosomes Cancer* **34**, 48–57.

[20] Stephan EA, Chung TH, Grant CS, Kim S, Von Hoff DD, Trent JM, and Demeure MJ (2008). Adrenocortical carcinoma survival rates correlated to genomic copy number variants. *Mol Cancer Ther* **7**, 425–431.

[21] Szabo PM, Tamasi V, Molnar V, Andrasfalvy M, Tombol Z, Farkas R, Kovesdi K, Patocs A, Toth M, Szalai C, et al. (2010). Meta-analysis of adrenocortical tumour genomics data: novel pathogenic pathways revealed. *Oncogene* **29**, 3163–3172.

[22] LaFramboise T (2009). Single nucleotide polymorphism arrays: a decade of biological, computational and technological advances. *Nucleic Acids Res* **37**, 4181–4193.

[23] Bignell GR, Huang J, Greshock J, Watt S, Butler A, West S, Grigorova M, Jones KW, Wei W, Stratton MR, et al. (2004). High-resolution analysis of DNA copy number using oligonucleotide microarrays. *Genome Res* **14**, 287–295.

[24] Dutt A and Beroukhim R (2007). Single nucleotide polymorphism array analysis of cancer. *Curr Opin Oncol* **19**, 43–49.

[25] Nieman LK, Biller BM, Findling JW, Newell-Price J, Savage MO, Stewart PM, and Montori VM (2008). The diagnosis of Cushing's syndrome: an Endocrine Society Clinical Practice Guideline. *J Clin Endocrinol Metab* **93**, 1526–1540.

[26] Fassnacht M, Beuschlein F, Quinkler M, and Petersenn S (2010). Arterial hypertension and subclinical Cushing's syndrome [in German]. *MMW Fortschr Med* **152**, 39–41.

[27] Cheung KJ, Delaney A, Ben-Neriah S, Schein J, Lee T, Shah SP, Cheung D, Johnson NA, Mungall AJ, Telenius A, et al. (2010). High resolution analysis of follicular lymphoma genomes reveals somatic recurrent sites of copy-neutral loss of heterozygosity and copy number alterations that target single genes. *Genes Chromosomes Cancer* **49**, 669–681.

[28] Choy KW, Setlur SR, Lee C, and Lau TK (2010). The impact of human copy number variation on a new era of genetic testing. *BJOG* **117**, 391–398.

[29] Benjamini Y and Hochberg Y (1995). Controlling the false discovery rate—a practical and powerful approach to multiple testing. *J R Stat Soc B Met* **57**, 289–300.

[30] Jensen LJ, Kuhn M, Stark M, Chaffron S, Creevey C, Muller J, Doerks T, Julien P, Roth A, Simonovic M, et al. (2009). STRING 8—a global view on proteins and their functional interactions in 630 organisms. *Nucleic Acids Res* **37**, D412–D416.

[31] Szklarczyk D, Franceschini A, Kuhn M, Simonovic M, Roth A, Minguez P, Doerks T, Stark M, Muller J, Bork P, et al. (2011). The STRING database in 2011: functional interaction networks of proteins, globally integrated and scored. *Nucleic Acids Res* **39**, D561–D568.

[32] Haralambieva E, Kleiverda K, Mason DY, Schuuring E, and Kluin PM (2002). Detection of three common translocation breakpoints in non–Hodgkin's lymphomas by fluorescence *in situ* hybridization on routine paraffin-embedded tissue sections. *J Pathol* **198**, 163–170.

[33] LeBron C, Pal P, Brait M, Dasgupta S, Guerrero-Preston R, Looijenga LH, Kowalski J, Netto G, and Hoque MO (2011). Genome-wide analysis of genetic alterations in testicular primary seminoma using high resolution single nucleotide polymorphism arrays. *Genomics* **97**, 341–349.

[34] Toma MI, Grosser M, Herr A, Aust DE, Meye A, Hoefling C, Fuessel S, Wuttig D, Wirth MP, and Baretton GB (2008). Loss of heterozygosity and copy number abnormality in clear cell renal cell carcinoma discovered by high-density Affymetrix 10K single nucleotide polymorphism mapping array. *Neoplasia* **10**, 634–642.

[35] Chari R, Coe BP, Vucic EA, Lockwood WW, and Lam WL (2010). An integrative multi-dimensional genetic and epigenetic strategy to identify aberrant genes and pathways in cancer. *BMC Syst Biol* **4**, 67.

[36] Pfaffl MW (2001). A new mathematical model for relative quantification in real-time RT-PCR. *Nucleic Acids Res* **29**, e45.
[37] Sbiera S, Schmull S, Assie G, Voelker HU, Kraus L, Beyer M, Ragazzon B, Beuschlein F, Willenberg HS, Hahner S, et al. (2010). High diagnostic and prognostic value of steroidogenic factor-1 expression in adrenal tumors. *J Clin Endocrinol Metab* **95**, E161–E171.
[38] Lobry C, Oh P, and Aifantis I (2011). Oncogenic and tumor suppressor functions of Notch in cancer: it's NOTCH what you think. *J Exp Med* **208**, 1931–1935.
[39] Almeida MQ, Fragoso MC, Lotfi CF, Santos MG, Nishi MY, Costa MH, Lerario AM, Maciel CC, Mattos GE, Jorge AA, et al. (2008). Expression of insulin-like growth factor-II and its receptor in pediatric and adult adrenocortical tumors. *J Clin Endocrinol Metab* **93**, 3524–3531.
[40] Yashiro T, Hara H, Fulton NC, Obara T, and Kaplan EL (1994). Point mutations of *ras* genes in human adrenal cortical tumors: absence in adrenocortical hyperplasia. *World J Surg* **18**, 455–460; discussion 460-451.
[41] Patterson EE, Holloway AK, Weng J, Fojo T, and Kebebew E (2011). MicroRNA profiling of adrenocortical tumors reveals miR-483 as a marker of malignancy. *Cancer* **117**, 1630–1639.
[42] Schmitz KJ, Helwig J, Bertram S, Sheu SY, Suttorp AC, Seggewiss J, Willscher E, Walz MK, Worm K, and Schmid KW (2011). Differential expression of microRNA-675, microRNA-139-3p and microRNA-335 in benign and malignant adrenocortical tumours. *J Clin Pathol* **64**, 529–535.
[43] Pasquale EB (2010). Eph receptors and ephrins in cancer: bidirectional signalling and beyond. *Nat Rev Cancer* **10**, 165–180.
[44] El Wakil A and Lalli E (2011). The Wnt/β-catenin pathway in adrenocortical development and cancer. *Mol Cell Endocrinol* **332**, 32–37.
[45] Artunc F, Sandulache D, Nasir O, Boini KM, Friedrich B, Beier N, Dicks E, Potzsch S, Klingel K, Amann K, et al. (2008). Lack of the serum and glucocorticoid-inducible kinase SGK1 attenuates the volume retention after treatment with the PPARγ agonist pioglitazone. *Pflugers Arch* **456**, 425–436.
[46] Amato R, D'Antona L, Porciatti G, Agosti V, Menniti M, Rinaldo C, Costa N, Bellacchio E, Mattarocci S, Fuiano G, et al. (2009). Sgk1 activates MDM2-dependent p53 degradation and affects cell proliferation, survival, and differentiation. *J Mol Med (Berl)* **87**, 1221–1239.
[47] Lang F, Perrotti N, and Stournaras C (2010). Colorectal carcinoma cells—regulation of survival and growth by SGK1. *Int J Biochem Cell Biol* **42**, 1571–1575.
[48] Reiter MH, Vila G, Knosp E, Baumgartner-Parzer SM, Wagner L, Stalla GK, and Luger A (2011). Opposite effects of serum- and glucocorticoid-regulated kinase-1 and glucocorticoids on POMC transcription and ACTH release. *Am J Physiol Endocrinol Metab* **301**, E336–E341.
[49] Miyata S, Koyama Y, Takemoto K, Yoshikawa K, Ishikawa T, Taniguchi M, Inoue K, Aoki M, Hori O, Katayama T, et al. (2011). Plasma corticosterone activates SGK1 and induces morphological changes in oligodendrocytes in corpus callosum. *PLoS One* **6**, e19859.
[50] Lang F, Bohmer C, Palmada M, Seebohm G, Strutz-Seebohm N, and Vallon V (2006). (Patho)physiological significance of the serum- and glucocorticoid-inducible kinase isoforms. *Physiol Rev* **86**, 1151–1178.
[51] Tyybakinoja A, Elonen E, Vauhkonen H, Saarela J, and Knuutila S (2008). Single nucleotide polymorphism microarray analysis of karyotypically normal acute myeloid leukemia reveals frequent copy number neutral loss of heterozygosity. *Haematologica* **93**, 631–632.
[52] Hayward P, Brennan K, Sanders P, Balayo T, DasGupta R, Perrimon N, and Martinez Arias A (2005). Notch modulates Wnt signalling by associating with Armadillo/β-catenin and regulating its transcriptional activity. *Development* **132**, 1819–1830.
[53] Balint K, Xiao M, Pinnix CC, Soma A, Veres I, Juhasz I, Brown EJ, Capobianco AJ, Herlyn M, and Liu ZJ (2005). Activation of Notch1 signaling is required for β-catenin–mediated human primary melanoma progression. *J Clin Invest* **115**, 3166–3176.
[54] Failor KL, Desyatnikov Y, Finger LA, and Firestone GL (2007). Glucocorticoid-induced degradation of glycogen synthase kinase-3 protein is triggered by serum- and glucocorticoid-induced protein kinase and Akt signaling and controls β-catenin dynamics and tight junction formation in mammary epithelial tumor cells. *Mol Endocrinol* **21**, 2403–2415.
[55] Mo JS, Ann EJ, Yoon JH, Jung J, Choi YH, Kim HY, Ahn JS, Kim SM, Kim MY, Hong JA, et al. (2011). Serum- and glucocorticoid-inducible kinase 1 (SGK1) controls Notch1 signaling by downregulation of protein stability through Fbw7 ubiquitin ligase. *J Cell Sci* **124**, 100–112.

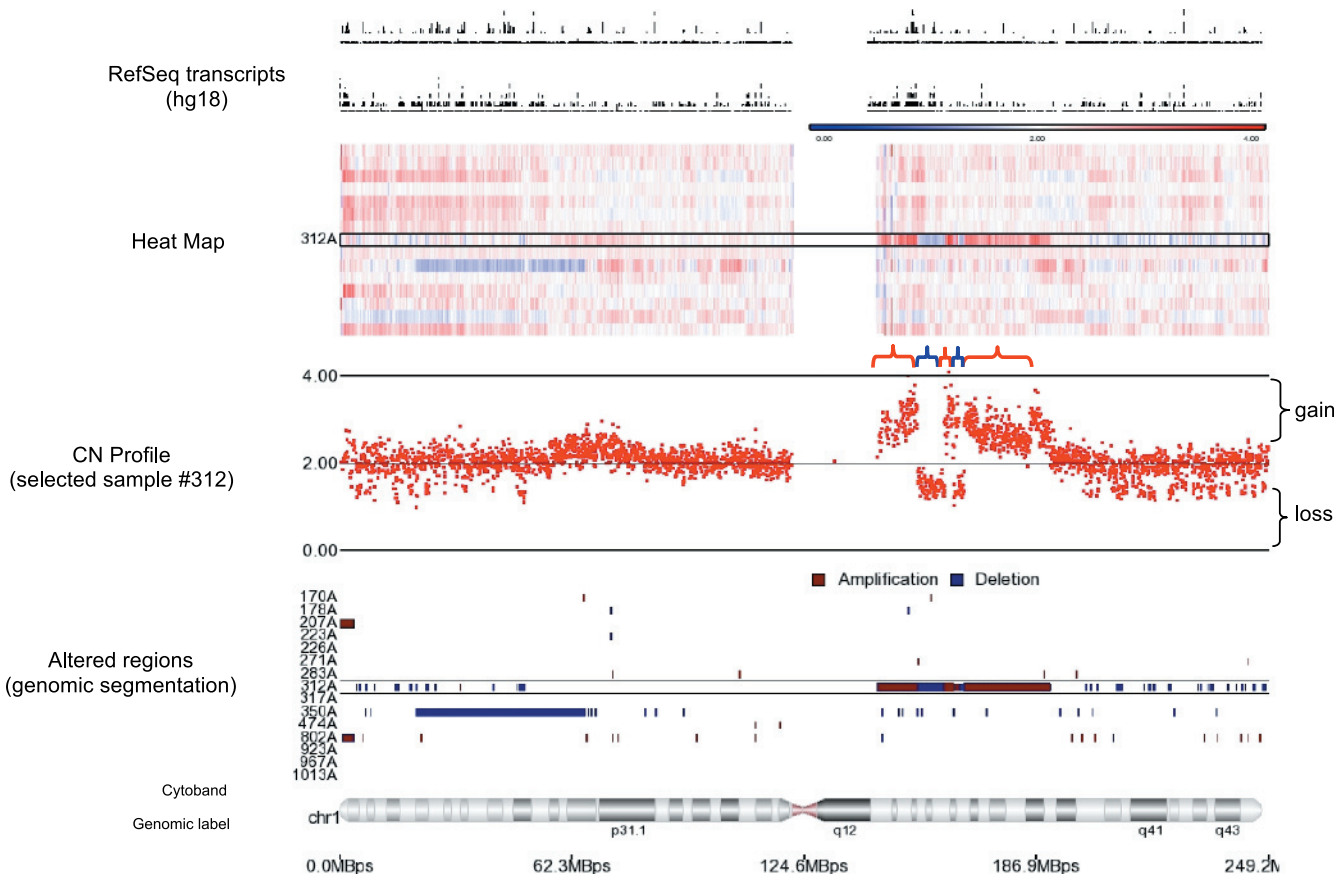

Figure W1. Chromosomal view of one representative chromosome (chr 1) in 15 cortisol-secreting ACA. The heat map shows the intensity plots in each sample. Gains/amplifications are represented in red and losses/deletions in blue. The CN profile is shown for one representative case (no. 312A). Normal CN score corresponds to 2.0, whereas gains correspond to a CN score greater than 2.5 and losses to a CN score less than 1.5 in blue. The genomic segmentation (Partek GS) shows the altered regions for each sample (selected case underlined). CN gains are represented in red and CN losses in blue.

Table W1. Primers for RT-qPCR at the DNA Level (Validation) and at the mRNA Level (Gene Expression) for the Candidate Genes and for the Internal Reference Genes.

DNA RT-qPCR

Gene Symbol		Primers	Chromosome
IGF2	fw	5′-gct gac acc tgg cgg cca tt-3′	11
	rw	5′-ggc gtc ctg act ttg ccc cc-3′	
EPHA7	fw	5′-agg cct tgg cca gga agc tg-3′	6
	rw	5′-ggc ttg cac ata tcc ctt ctg ccc-3′	
SGK1	fw	5′-tgg aag ctg ctg ctg ccc ac-3′	6
	rw	5′-tgt cca tct ctg gcc ccc gg-3′	
CTNNB1	fw	5′-acg agg agg caa gtt tct cca agg-3′	3
	rw	5′-tgc gcc tct ccc cac ctc ac-3′	
CYP11B2	fw	5′-cct gtg tct tgg ggc gg-3′	8
	rw	5′-ggc ctt ggg cga cag cac at-3′	
GAPDH	fw	5′-tga cgc tgg ggc tgg cat tg-3′	12
	rw	5′-ggc ggc aga ccc tgc act tt-3′	

RNA RT-qPCR

Gene Symbol	Primer Probe Mix*	Chromosome	Amplicon Length (bp)
IGF2	Hs00171254_m1	11	94
EPHA7	Hs01033009_m1	6	88
SGK1	Hs00178612_m1	6	81
CTNNB1	Hs00994404_g1	3	93
FHIT	Hs00179987_m1	3	79
NOTCH1	Hs01062014_m1	9	80
CYP11B1	Hs01596404_m1	8	137
CYP11B2	Hs01597732_m1	8	137
HRAS	Hs00610483_m1	11	69
β-actin	Hs9999903_m1	7	171

*TaqMan Gene Expression Assays (Applied Biosystems).

Table W4. Gene Ontology Family Analysis (Performed with GSEA) Including the Genes with CNAs Observed in at Least 2 of 15 Cortisol-Secreting ACAs (Frequency, ≥13%; Total, 638 Recognized Genes).

Cytokines and Growth Factors	Transcriptional Factors	Homeodomain Proteins	Cell Differentiation Markers	Protein Kinases	Oncogenes	Tumor Suppressor Genes
CTGF	*IRX4*	*IRX4*	***CD151***	***ADCK5***	*CTNNB1*	***FANCA***
IGF2	***LHX3***	***LHX3***	*CD24*	*BRSK2*	*DUX4*	*RECQL4*
INS	*NKX6-2*	*NKX6-2*	*IFITM1*	*CAMK2B*	***HRAS***	*TSC2*
INS-IGF2	*TGIF1*	*TGIF1*	*IL9R*	*CDK10*	***NOTCH1***	*FHIT*
KITLG	*VENTX*	*TGIF2LY*	***L1CAM***	*CDK11A*	*PRDM16*	***H19***
PDGFA	*CTNNB1*	***UNCX***	*RHCE*	***EPHA7***	*STIL*	
SCT	*DUX4*	*VENTX*	*TNFRSF4*	*EPHB2*		
SLURP1	*PRDM16*			***IRAK1***		
	ARC			***MAPK15***		
	DEAF1			*NRBP2*		
	E2F2			*PRKCZ*		
	E4F1			*PRKG1*		
	FAM20C			*PRKY*		
	FOXH1			*PTK2*		
	HES4			*SGK1*		
	HES5					
	HEY2					
	HSF1					
	HSFY1					
	ID3					
	IRF7					
	LRRC14					
	MAFK					
	MECP2					
	MFSD3					
	NFKBIL2					
	NPAS2					
	PHRF1					
	PRDM7					
	RASSF7					
	REV3L					
	RXRA					
	SCRT1					
	SNAPC4					
	SOX8					
	SRY					
	TBL1Y					
	TP73					
	TRIP13					
	UTF1					
	ZFY					
	ZNF16					
	ZNF250					
	ZNF251					
	ZNF33B					
	ZNF696					
	ZNF7					

Red: genes with CN gains
Blue: genes with CN losses.
Underlined: genes with microalterations.
Bold: genes altered in at least three samples (frequency, ≥20%).

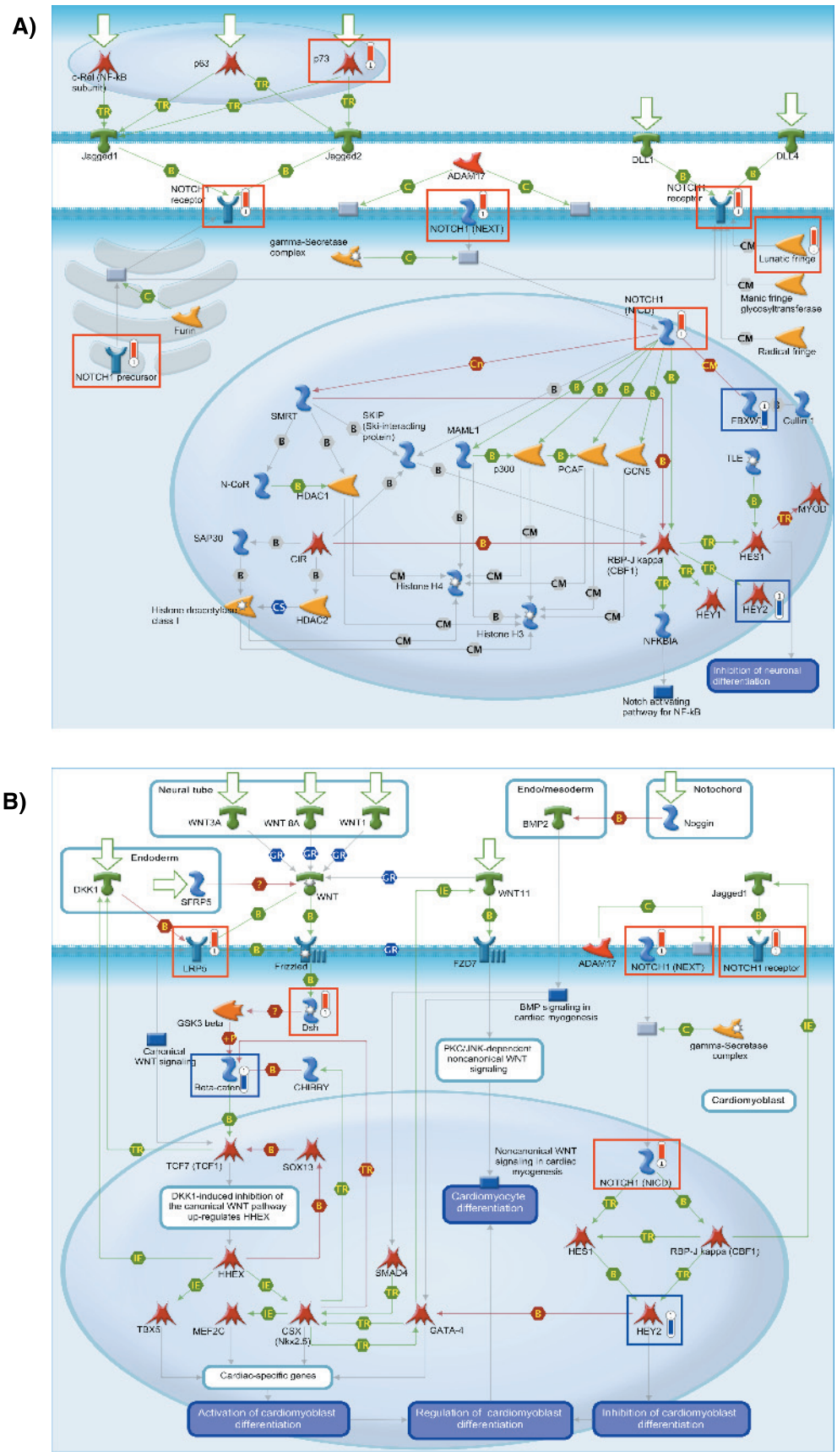

Figure W2. The Notch signaling pathway map (A, gene ontology enrichment $P = 1.494^{e-6}$) and the Wnt and Notch signaling in early cardiac myogenesis (B, gene ontology enrichment, $P = 4.287^{e-6}$) according to the GeneGo analysis (MetaCore Analytical suite) including all the genes ($n = 285$ annotated genes) with CNAs observed in at least two samples (recurrent CNA). Genes with gains are underlined in red and genes with losses in blue. Detailed legend is available at http://www.genego.com/mapsearch.php.

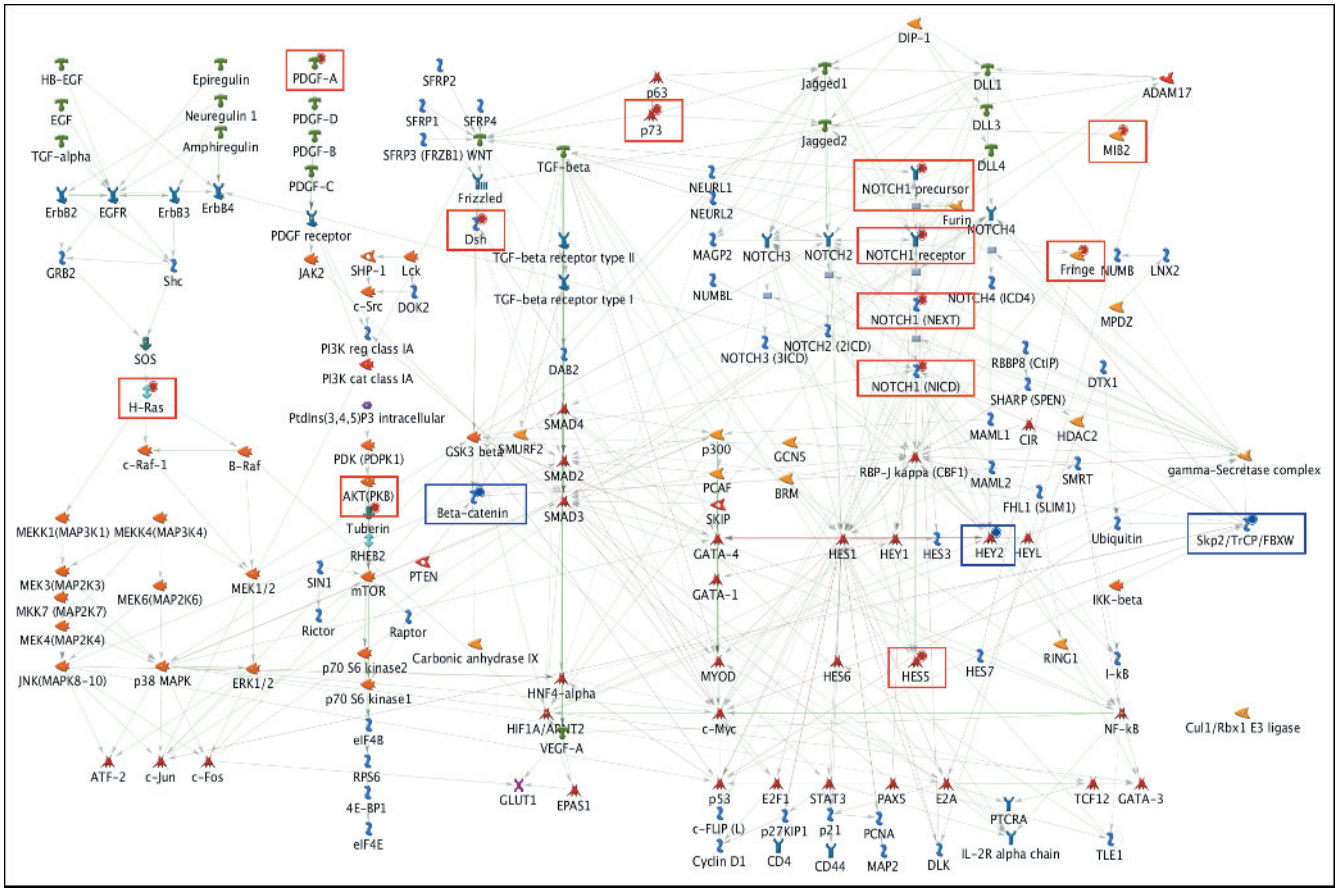

Figure W3. The entire Notch signaling gene network according to the GeneGo analysis (MetaCore Analytical suite). Detailed legend is available at http://www.genego.com/mapsearch.php.

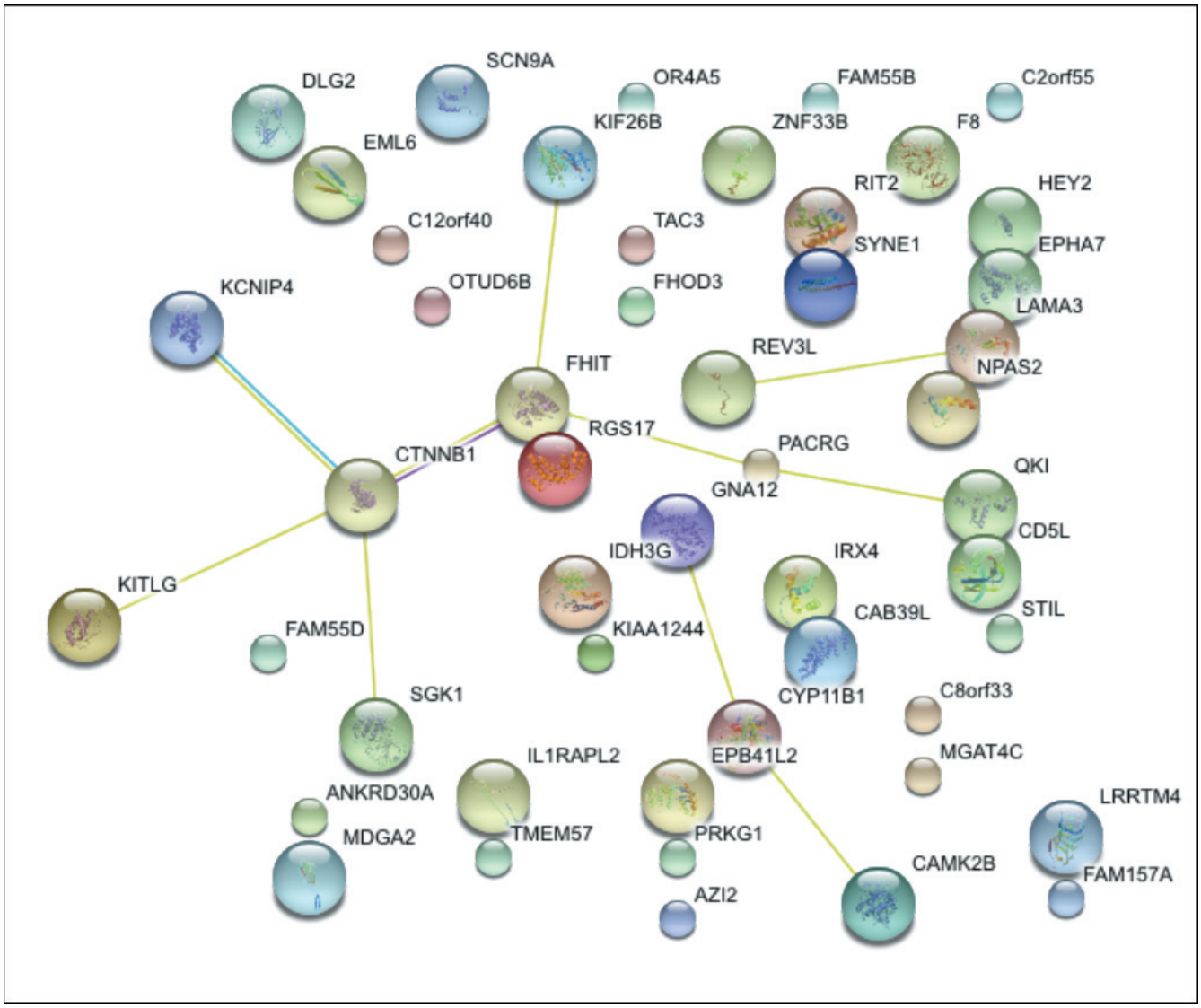

Figure W4. Graphical representation of the STRING-generated protein-protein network (action view) for the single genes with CN micro-alterations observed in at least two samples ($n = 46$ annotated genes). Modes of action are shown in different colors. Detailed legend is available at http://string-db.org/newstring_cgi/show_network_section.